

# Diel and seasonal methane dynamics in the shallow and turbulent Wadden Sea

Tim R. de Groot <sup>1</sup>, Anne M. Mol <sup>1</sup>, Katherine Mesdag <sup>2</sup>, Pierre Ramond <sup>1,3</sup>, Rachel Ndhlovu <sup>1</sup>, Julia C. Engelmann <sup>1</sup>, Thomas Röckmann <sup>2</sup> and Helge Niemann <sup>1,4,5</sup>

1. Royal Netherlands Institute for Sea Research (NIOZ), Texel, the Netherlands

2. Institute for Marine and Atmospheric Research Utrecht (IMAU), Utrecht University, Utrecht, The Netherlands

3. Instituto de Ciencias del Mar (ICM), Barcelona, Spain

4. Department of Earth Sciences, Utrecht University, Utrecht, The Netherlands

5. Centre of Arctic Gas Hydrate, Environment and Climate (CAGE), UiT the Arctic University of Norway, Tromsø, Norway

Correspondence to: Tim de Groot (tim.de.groot@nioz.nl)

## This file includes:

Supplementary materials and methods

Fig. S1. Concentrations of methane in sediments at time-series station

Fig. S2. Isotope fractionation

Fig. S3. Pearson correlation matrix for variables used in PCA

Table S1. Statistical comparison between tidal phases

Table S2. Principal component analysis loadings

## Supplementary materials and methods

*Endmember mixing modelling* – Linear mixing of surface waters equilibrated with atmospheric CH<sub>4</sub> and bottom waters with maximum methane concentrations was modelled based on an endmember approach. Equilibrium with atmospheric methane was assumed for surface waters translating to CH<sub>4</sub> concentrations of ~ 3 nM (Wiesenberg and Guinasso, 1979) with a δD-value of ~ -85 ‰ (Whiticar, 1999). The second endmember was water with maximum CH<sub>4</sub> concentration in autumn at 3 m water depth at 0 h (i.e., 35.5 nM, δD-CH<sub>4</sub> = -254 ‰) and in summer at 3 m water depth at 36 h (i.e., 154.9 nM, δD-CH<sub>4</sub> = -250 ‰).

*Rayleigh fractionation modelling* - A Rayleigh fractionation model was constructed for hydrogen stable isotope compositions to test whether the enrichment in heavy isotopes (D) at low CH<sub>4</sub> concentrations was related to methane oxidation by methanotrophs (Whiticar, 1999). For this, samples with methane concentrations < 21 nM (δD-CH<sub>4</sub> = ~ -217 ‰) in autumn and < 61 nM (δD-CH<sub>4</sub> = ~ -244 ‰) in summer were defined as the methane source signal and thus the starting point of the Rayleigh fractionation model. These values were chosen because above these concentrations, the isotope effect imposed by MOx is masked by the high background CH<sub>4</sub> and/or is overprinted by methane entering the water column from sediments. The apparent isotope enrichment ε is then calculated according to an open system approach (Mariotti et al., 1981; Jacques et al., 2021):

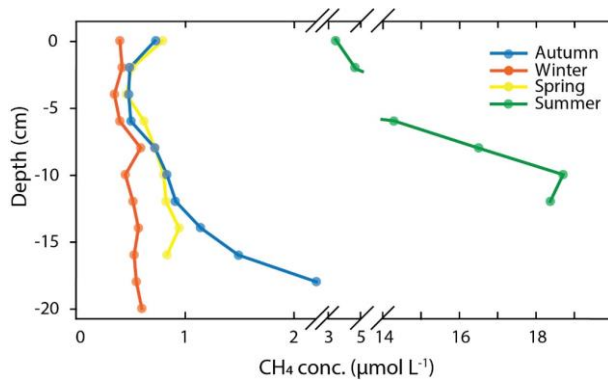
$$\delta_s = \delta_{s,0} + \epsilon_{\text{open}} \ln f \quad (6)$$

Where δ<sub>s</sub> and δ<sub>s,0</sub> are the δD values of methane at a given concentration and of the source signal, respectively. *f* denotes the fraction of the remaining methane. Apparent ε-values for δD-CH<sub>4</sub> were -97.26 ‰ in autumn (Fig. S2) and comparable to previous reported fractionation factor (Jacques et al., 2021). Note that for δD-CH<sub>4</sub> in summer,

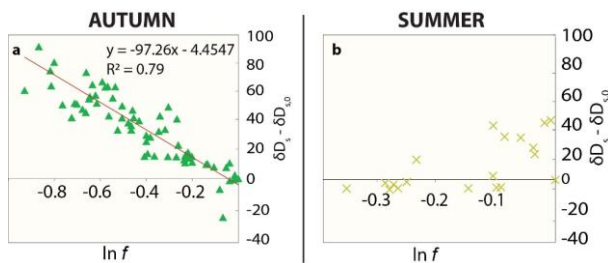
44 there was no heavy isotope enrichment, precluding to calculate Rayleigh distillation for H/D in a well constrained  
 45 manner.

46 **Supplementary figures and tables**

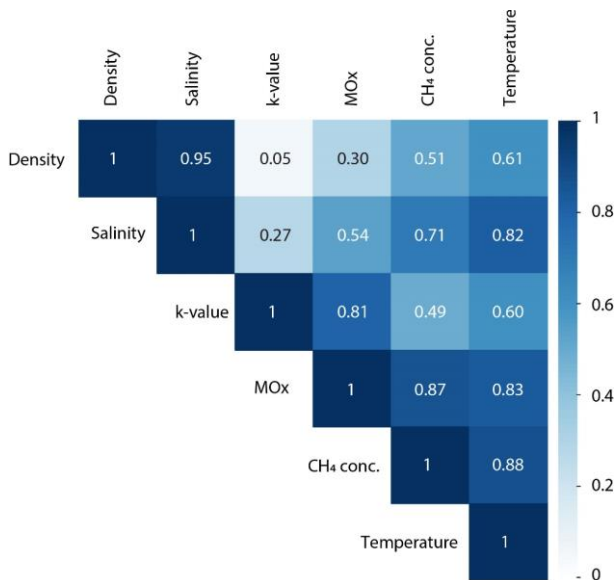
47



48  
 49 **Figure S1.** Concentrations of methane in sediments at the time-series station.



50  
 51 **Figure S2.** Rayleigh fractionation of stable hydrogen isotopes in (A) autumn and (B) summer. Samples with methane  
 52 concentrations < 21 nM ( $\delta\text{D}-\text{CH}_4 \approx -217\%$ ) in autumn and < 61 nM ( $\delta\text{D}-\text{CH}_4 \approx -244\%$ ) in summer were defined as the  
 53 methane source signal ( $\text{CH}_{4(0)}$ ,  $\delta_0$ ). The apparent isotope enrichment  $\epsilon$  was then calculated according to an open system  
 54 approach. Note that  $\delta\text{D}-\text{CH}_4$  values did not deviate consistently with methane concentrations <61 nM, precluding to  
 55 calculate Rayleigh distillation for H/D in a well constrained manner.



56  
 57 **Figure S3.** Pearson correlation matrix depicting the correlations between variables used in a principal component analysis.

58

59 **Table S1.** Differences in methane concentration,  $k$ , and MOx between tidal phases. Welch's t-test was applied to methane  
 60 concentrations, first order rate constants and MOx at low tide and high tide. p-values marked in grey indicate non-significant  
 61 differences ( $p > 0.05$ ).

Season	Variable	LT (n)	HT (n)	Increase at LT vs. HT	Welch's t-test P(T<=t) two-tail
Autumn	CH <sub>4</sub> conc.	10	8	21%	0.34
Winter	CH <sub>4</sub> conc.	8	5	3%	0.47
Spring	CH <sub>4</sub> conc.	8	6	25%	0.13
Summer	CH <sub>4</sub> conc.	8	8	2%	0.94
Autumn	$k$	10	8	76%	0.003
Winter	$k$	8	5	8%	0.83
Spring	$k$	8	6	259%	$5.5 \times 10^{-5}$
Summer	$k$	8	8	30%	0.07
Autumn	MOx	10	8	208%	0.03
Winter	MOx	8	5	9%	0.82
Spring	MOx	8	6	345%	$6.4 \times 10^{-6}$
Summer	MOx	8	8	24%	0.38

62  
 63 **Table S2.** Contribution of individual variables to the principal components. Variables are centred and scaled before running  
 64 PCA.

	PC 1	PC 2	PC 3	PC 4	PC 5
CH <sub>4</sub> conc.	20.1	0.49	40.34	6.57	32.49
$k$	9.72	32.51	42.77	0.55	14.43
MOx	18.5	14.13	2.41	13.09	15.79
Density	11.38	35.27	10.17	11.82	0.03
Temperature	22.31	0.02	0.72	67.72	0.87
Salinity	17.99	17.57	3.58	0.24	0.39

65

## 66 References

- 67 Jacques, C., Gkritzalis, T., Tison, J.-L., Hartley, T., van der Veen, C., Röckmann, T., Middelburg, J. J.,  
 68 Cattrijsse, A., Egger, M., Dehairs, F., and Sapart, C. J.: Carbon and Hydrogen Isotope Signatures of Dissolved  
 69 Methane in the Scheldt Estuary, *Estuaries and Coasts*, 44, 137-146, 10.1007/s12237-020-00768-3, 2021.  
 70 Mariotti, A., Germon, J. C., Hubert, P., Kaiser, P., Letolle, R., Tardieux, A., and Tardieux, P.: Experimental  
 71 determination of nitrogen kinetic isotope fractionation: Some principles; illustration for the denitrification and  
 72 nitrification processes, *Plant and Soil*, 62, 413-430, 10.1007/BF02374138, 1981.  
 73 Whiticar, M. J.: Carbon and hydrogen isotope systematics of bacterial formation and oxidation of methane,  
 74 *Chemical Geology*, 161, 291-314, [https://doi.org/10.1016/S0009-2541\(99\)00092-3](https://doi.org/10.1016/S0009-2541(99)00092-3), 1999.  
 75 Wiesenberg, D. A. and Guinasso, N. L.: Equilibrium Solubilities of Methane, Carbon Monoxide, and Hydrogen  
 76 in Water and Sea Water, *Journal of Chemical & Engineering Data*, 24, 356-360, 1979.

77